

VYSOKÉ UČENÍ TECHNICKÉ V BRNĚ
BRNO UNIVERSITY OF TECHNOLOGY

FAKULTA strojního inženýrství
ÚSTAV fyzikálního inženýrství

Faculty of mechanical Engineering
Institute of Physical Engineering

ING. PAVEL URBAN

Heliový kryostat pro studium turbulentního proudění při přirozené konvekci
Helium Cryostat for Experimental Study of Natural Turbulent Convection
Zkrácená verze PhD Thesis

Obor: Fyzikální a materiálové inženýrství
Školitel: RNDr. Věra Musilová, CSc.
Školitel specialista: prof. RNDr. Ladislav Skrbek, DrSc.
Datum obhajoby:

Keywords

helium cryostat, turbulent flow, natural convection, Rayleigh-Bénard convection, heat transfer, Rayleigh number

Klíčová slova

heliový kryostat, turbulentní proudění, přirozená konvekce, Rayleigh-Bénardova konvekce, přenos tepla, Rayleighovo číslo

Disertační práce je uložena na – doplní redakce

údaje o copyrightu, ISBN (80-214 - doplní redakce) a ISSN (1213-4198)

Contents

1	THE STATE-OF-ART	5
1.1	Introduction.....	5
1.2	Scaling laws of natural convection	6
1.2.1	<i>Nu(Ra) dependence</i>	6
1.2.2	<i>Kraichnan regime</i>	6
1.3	Experiments	7
1.3.1	<i>Laboratory model of RBC</i>	7
1.3.2	<i>Helium as a working fluid</i>	7
1.3.3	<i>Contradictory experimental results</i>	7
1.3.4	<i>Parasitic heat fluxes</i>	8
1.3.5	<i>Effect of plates on convection</i>	8
2	OBJECTIVES AND METHODS	9
2.1	Objectives.....	9
2.2	Methods.....	9
3	APPARATUS DESCRIPTION.....	9
3.1	Cryostat conception.....	10
3.2	Convection cell conception.....	11
3.2.1	<i>Sidewalls of the cell</i>	12
3.2.2	<i>Copper plates</i>	12
3.2.3	<i>Construction joints and the technology</i>	13
4	ANALYSIS OF THE CONVECTION EXPERIMENT	13
4.1	Measurement of <i>Nu(Ra)</i> dependence	13
4.1.1	<i>Measured quantities</i>	14
4.1.2	<i>Total accuracy assessment</i>	14
4.2	Model of the experiment	16
4.2.1	<i>Results of the analysis</i>	16
4.3	Heat flux analysis of the cryostat.....	20
5	REALIZATION OF THE CRYOSTAT	21
5.1	The convection cell	21
5.2	LHe vessel.....	22
5.3	Cryostat assembly	24
6	CONCLUSIONS	25
7	REFERENCES	26
8	CURRICULUM VITAE	29

1 THE STATE-OF-ART

1.1 INTRODUCTION

Turbulent natural convection plays a prominent role in heat transport phenomena such as atmospheric and oceanic circulation, geodynamics, stellar convection and relevant industrial applications.

As a fundamental theory based on first principles is absent, dimensionless numbers and phenomenological analyses are generally used to describe fluid flows. The most relevant issue is then to estimate the corresponding scaling laws. Without their knowledge, scaling-up from laboratory models to actual processes is not possible. Many researchers are consequently performing experiments and computations worldwide to gain a better understanding of turbulent convection and are engaged in lively discussions on controversial outcomes.

The simplest configuration of natural convection is known as the Rayleigh-Bénard convection (RBC). It is defined as a thermally driven flow in a fluid layer between two infinite rigid horizontal plates, where constant temperatures are imposed on both fluid boundaries [1]. The bottom plate is heated and the top one is cooled. The basic issue is to find a relation between the heat flux density H transferred by convection and the temperature difference ΔT between the bottom and top plates.

The convection heat transfer can be characterised by the Nusselt number Nu

$$Nu = \frac{H}{H_0} = \frac{L \cdot H}{\lambda \cdot \Delta T}, \quad (1)$$

representing a dimensionless ratio of the measured density of the heat flux H to the conductive density of the heat flux $H_0 = \lambda \Delta T / L$, that would occur in the fluid without motion. Here λ is the heat conductivity of the fluid and L is the height of the fluid layer.

From the dimensional analysis of the mass, momentum and energy conservation equations of an almost incompressible fluid (Boussinesq approximation), it follows that the description of the RBC depends on two dimensionless parameters. These are the Rayleigh number Ra ,

$$Ra = \frac{g \cdot \alpha \cdot \Delta T \cdot L^3}{\nu \cdot \kappa} \quad (2)$$

and Prandtl number Pr ,

$$Pr = \frac{\nu}{\kappa}, \quad (3)$$

where g is the gravity acceleration, α , ν and κ are the isobaric thermal expansion coefficient, kinematic viscosity and thermal diffusivity, respectively. The onset of the RBC between infinite plates is theoretically predicted for the critical Rayleigh number $Ra_c = 1708$ which agrees with its experimental value.

The Boussinesq condition

$$\alpha \cdot \Delta T \ll 1 \quad (4)$$

justifies the assumption of “incompressibility” of the working fluid in experiments with gaseous fluids [1]. Variations of the density are only a source of buoyancy force in this approximation.

1.2 SCALING LAWS OF NATURAL CONVECTION

1.2.1 $Nu(Ra)$ dependence

The Rayleigh-Bénard convection is a model for fundamental convection studies [1]. The fluid layer becomes turbulent typically at Rayleigh numbers Ra exceeding 10^5 , except for the boundary layer. In experiments on the RBC in turbulent regime a power law is obtained, that is

$$Nu \sim Ra^\gamma, \quad (5)$$

where γ is usually close to $1/3$.

The power law with γ close to $1/3$ corresponds to a simplified model of convection, where all the temperature difference ΔT drops on the boundary layers (thin in comparison with L) while the central turbulent fluid is effectively mixed and has a nearly constant temperature. Heat transfer is thus controlled by heat conduction of the boundary layers and convective heat flux does not consequently depend on the height L of the fluid. This fact explicates the $\gamma = 1/3$ power law.

1.2.2 Kraichnan regime

Turbulence effects start to be independent on the fluid viscosity when the fluid velocity is sufficiently large, i.e. when viscous damping is negligible in comparison with flow inertia. In natural convection this assumption results in the relation

$$Nu \sim Ra^{1/2} \quad (6)$$

for high Ra (for high driving buoyancy force) [2].

This regime is called the “ultimate regime” or “Kraichnan regime” and was first predicted by Kraichnan [3] for high values of Ra .

The boundary layer should undergo a laminar-turbulent transition for high Ra numbers and the heat flux is not anymore controlled by the laminar boundary layers in this regime.

Many large thermal circulations on the Earth, such as the atmospheric one, occur at high values of Ra , and are not easy or even impossible to be modelled in laboratory conditions. Unfortunately, discrepancies among experiments, results of numerical simulations, predictions on $Nu(Ra, Pr)$ dependence and onset of Kraichnan regime reveal a general lack of understanding. Experimental evidence of the predicted Kraichnan regime is thus of fundamental interest. In spite of considerable efforts, a convincing experiment that has unequivocally solved this question has yet to be performed [4], [5], [6].

1.3 EXPERIMENTS

1.3.1 Laboratory model of RBC

In laboratory conditions the RBC may be studied in a cylindrical cell with negligibly thermally conductive sidewalls, closed on its top and bottom sides by high heat conductivity and capacity plates. The geometry of the cell is characterized by the aspect ratio $\Gamma = D/L$, where L is the distance between the plates and D the inner diameter of the cell.

As mentioned above, the heat transferred by natural convection is given by a scaling relation $Nu = f(Ra, Pr)$ which in general depends also on the aspect ratio Γ .

1.3.2 Helium as a working fluid

Cryogenic helium (~ 5 K) is a useful working fluid for experimental studies of natural convection [7]. Helium properties have strong dependences on the pressure and temperature in the vicinity of the He critical point (5.195 K, 227.5 kPa and 69.64 kg/m^3) and cold helium gas has an extremely low viscosity and thermal diffusivity in comparison with other commonly used fluids (air, water, Hg) (Table 1).

Table 1 *Fluids properties*

Fluid	Temperature	$\alpha/\nu\text{K}$
Air	20 °C	0.122
Water	20 °C	14.4
Mercury	20 °C (SVP)	3.43
SF6	50 °C (5 MPa)	$7.5 \cdot 10^5$
Helium (gas)	5.5 K (280 kPa)	$1.41 \cdot 10^8$

This means that Ra number can be varied over a wide range of values and that it is also possible to reach simultaneously very high values of Ra in a relatively small cell filled with cold He gas. Niemela et al. [8] reached Ra of about 10^{17} , which is of the same order of magnitude as for atmospheric turbulence. Similar results can be achieved with the heavy gas SF_6 but disadvantage of this gas is the necessity of measurement at high pressures (up to 50 MPa at 300 K) for the highest Ra [9].

Another important advantage of using He as a working fluid is a very good knowledge of its thermophysical properties [10].

1.3.3 Contradictory experimental results

Evidence of transition towards the Kraichnan regime was claimed by the “Grenoble group” on the basis of experiments with cold He gas. Chavanne et al. [11] observed a power law $Nu \sim Ra^{0.38}$ and a different behaviour of the He temperature fluctuations above $Ra \sim 10^{11}$ in a cell with aspect ratio $\Gamma = \frac{1}{2}$ ($D = 100$ mm, $L = 200$ mm). This finding was interpreted as the transition to the Kraichnan regime

[5], [12], [13]. Recently Grenoble group [14], [15] repeated measurements with the cell used in previous experiments [13], but with improved thermometry. They confirmed results on $Nu(Ra)$ obtained by Chavanne et al. [13] with transition to a new regime at $Ra \sim 10^{11} - 10^{12}$.

On the other hand, the Oregon group (Niemela et al.) [8] published results for the same aspect ratio $\Gamma = 1/2$, but for a convection cell 5 times higher ($D = 0.5$ m, $L = 1$ m). They obtained the dependence $Nu \sim Ra^{0.309}$ in the Ra number range from 10^6 to 10^{17} without any evidence of transition to a different power law. Niemela and Sreenivasan [16], [17], performed additional experiments to check the dependence $Nu(Ra)$ with the aspect ratios $\Gamma = 1$ and 4. Also from those measurements, they obtained a power exponent close to $1/3$. In all experiments they measured temperature fluctuations at several positions inside the cell.

Concurrently with experiments, numerical simulations are being developed [4], [6], [18], [19], [20], [21]. This helps substantially to interpret experiments, and vice versa. Only experiments can confirm the numerical and theoretical models being developed.

1.3.4 Parasitic heat fluxes

Experimental data are influenced by the construction details of the cell, such as sidewall conduction, heat conductivity and capacity of the plates, surface roughness of the plates, etc. [17], [22], [23], [24]. Measured data have to be analyzed very carefully.

With increasing precision in the determination of Nusselt number Nu the spurious effects previously neglected have to be taken into account. It has been shown by a numerical model of Ahlers [22] that the conduction of the cell sidewalls may significantly contribute to heat transfer, increase the measured Nu value and thus influence the power law $Nu(Ra)$. Roche et al. [24] derived a simple analytical formula for the sidewall correction as a function of a so called wall number W . This is the ratio of the sidewall conductivity and conductivity of the static gas column in the cell.

The previous formula was tested by using the results obtained from three different cells with aspect ratio $1/2$: a large thick-wall cell with $W = 3$, a large thin-wall cell with $W = 0.6$ and a small cell, $W = 3$. After the correction, the data obtained from those cells collapsed within 15% error interval into one dependence $Nu(Ra)$ while the uncorrected data differed up to 40%.

1.3.5 Effect of plates on convection

Constant temperatures at the lower and upper He boundaries of the cell could be ideally maintained by top and bottom plates with infinite heat conductivity and capacity. The influence of the real properties of the plates was analyzed in [23]. According to the described analysis, the heat conductivity rather than the capacity of

the plates is crucial in experiments with He. The higher is the heat conductivity of the plate the less should be the plate effect on the convection.

2 OBJECTIVES AND METHODS

2.1 OBJECTIVES

The aim of the research project is to design, realize and test a helium cryostat with a cylindrical convection cell for investigation of the turbulent natural convection at high Rayleigh numbers ($10^6 < Ra < 10^{15}$). Cryogenic ^4He will be used as a working fluid. The work includes cryogenic tests and the preparation of the apparatus for the measurement of the functional dependence of the Nusselt number Nu on the Rayleigh number Ra .

As discussed above, various experiments with cryogenic ^4He gas gave controversial results. The cryostat is then to be designed for experiments which should resolve the question about the transition to an ultimate Kraichnan regime within a range of available Ra (sec. 1.2.2).

To achieve this goal the convection cell is to be designed with great emphasis on the minimum influence of the cell structure and materials on the studied convection within the considered wide range of Ra and Nu numbers.

2.2 METHODS

It is planned to employ know-how, equipment and technologies of the Institute of Scientific Instruments AS CR, v.v.i. (ISI):

1. The concept of the cryostat NMR III [25] developed at ISI is to be utilized. A newly designed experimental cell is to be implemented in the cryostat.
2. Special technologies of joining and welding (electron beam welding, vacuum brazing and microplasma welding) are at our disposal at ISI to design and manufacture the apparatus.
3. For the cryogenic tests, parts of an old experimental cryostat can be modified and reused.
4. Liquid helium (LHe) supply (recirculated in a recovery system) will be employed as the source of He.
5. For the experiment preparation (operating parameters of the working fluid, He consumption, duration of measurements, etc.) the NIST He database [10] will be used.

3 APPARATUS DESCRIPTION

3.1 CRYOSTAT CONCEPTION

The cryostat design is based on a low loss cryostats NMR III [25] for a NMR magnet developed and manufactured at ISI. In the centre of the cryostat (Figure 1), the experimental convection cell is placed instead of the superconducting magnet.

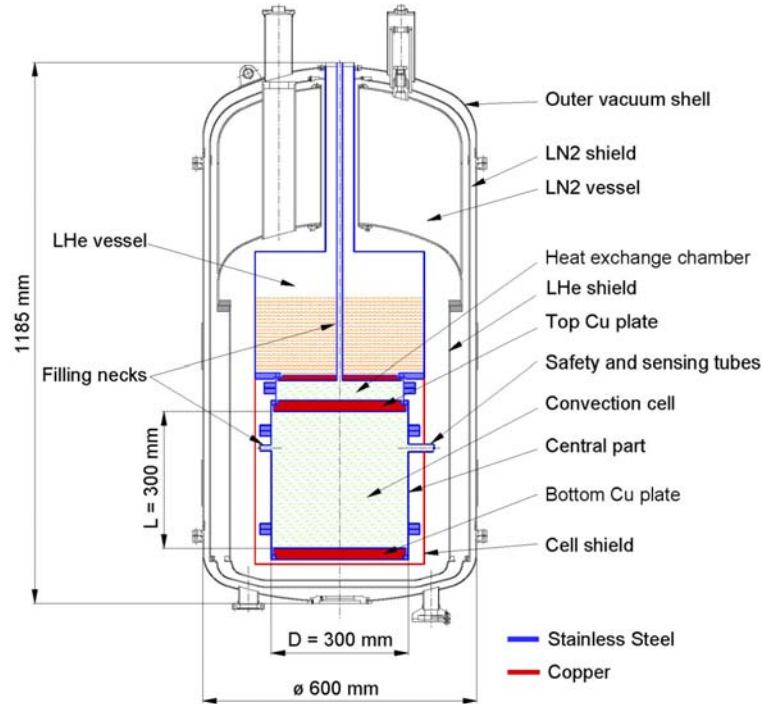


Figure 1 Schematic representation of the cryostat

The convection cell is thermally connected with a liquid helium vessel (LHe vessel) by a heat exchange chamber filled with gaseous He (GHe). The main function of the LHe vessel at 4.2 K in the cryostat is to remove the convection heat flux from the cell.

During all regimes of the experiment, total parasitic heat flux to the convection cell must be negligible in comparison with the measured convection heat flux. The contribution of thermal radiation to this parasitic heat is reduced by a cell radiation shield which is thermally anchored to the liquid He vessel.

In convection experiments the main heat load of the LHe vessel comes from the convection cell and this will be at least one order of magnitude higher than the LHe heat load typical for a NMR cryostat. Thus the LHe vessel and convection cell are shielded directly by the liquid nitrogen vessel (LN2 vessel) and LHe shield (~ 77 K), contrary to the low loss NMR cryostat, where another shield is inserted between the LHe and LN2 vessels. The radiation heat flux from the outer vacuum shell (300 K) to the LN2 vessel is reduced by a LN2 radiation shield (~ 220 K) that is cooled by cold gaseous nitrogen evaporated from the LN2 vessel.

The cell, heat exchange chamber and LHe vessel are suspended on a central neck inside the outer vacuum shell. High vacuum in the inner space of the cryostat

reduces heat fluxes by residual gas. The vacuum is maintained by cryopumping to a pressure lower than 10^{-6} Pa.

For most parts of the outer shell, LHe vessel, heat exchange chamber and convection cell austenitic stainless steel was used. The LN2 vessel and LN2 radiation shield are made of aluminium alloy, while for the protection of the cell a copper shield was designed.

3.2 CONVECTION CELL CONCEPTION

Target convection cell parameters

Ra number up to about 10^{15} under Boussinesq condition $\alpha \cdot \Delta T \leq 0.2$

- cylindrical experimental cell of 300 mm in diameter D and up to 300 mm in height L
- cylindrical cell with the top and bottom plates made of high conductivity copper
- sidewalls with low heat conductivity (to reduce substantially parasitic heat flux)
- the cell design allows to change the aspect ratio $\Gamma = D/L$ from 1 to 2.5 or to implement a middle part with a modified geometry
- operating pressures in the cell from 100 Pa to 250 kPa at temperatures from 4.2 K up to about 12 K
- electrical resistance heaters, placed in grooves on the plates, heat power from 10 mW to 10 W

The conception of the cylindrical convection cell is schematically shown in Figure 2. The convection cell is divided into three parts. The top and bottom parts are composed of thin stainless steel sidewalls of low heat conductivity and copper plates of high heat conductivity. The middle part is exchangeable and allows to vary the cell aspect ratio Γ .

A stainless steel tube is used for initial cooling procedure of the cell and for venting in the case of accidental overpressure. The second identical tube serves for pressure measurement and for venting of the cell.

The top and bottom plates are equipped with electrical resistance heaters. The bottom plate heater provides the cell with the convection heat flux. This flux is removed from the top plate of the cell via the heat exchange chamber. The top plate temperature is roughly set by gaseous He pressure in the chamber and the heater of the top plate serves for precise adjustment of this plate temperature.

The plates temperatures are measured by two sensors embedded near the inner surface of the plates.

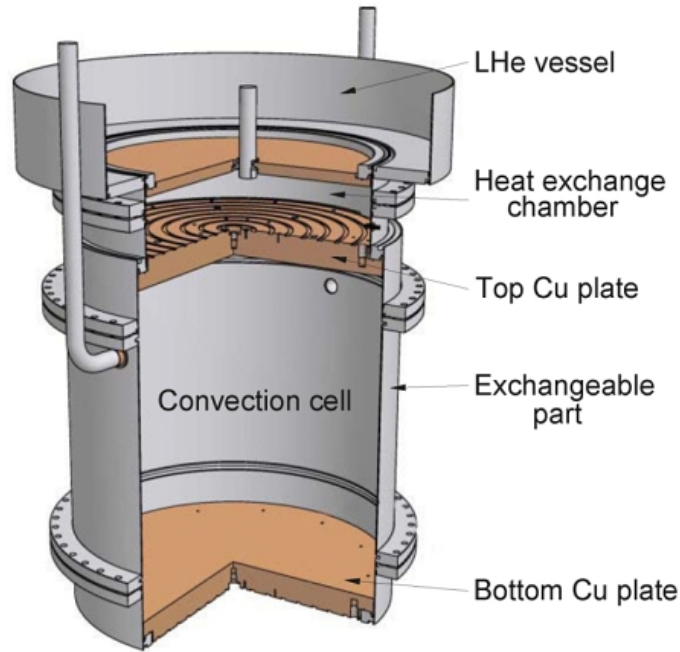


Figure 2 Three-dimensional section of the convection cell with the heat exchange chamber and part of the LHe vessel.

3.2.1 Sidewalls of the cell

The main temperature drop in the cell is on the fluid boundary layers and on the adjacent sidewalls. The height of the thin cylindrical sidewalls of the bottom and top parts should be higher at least than the supposed thickness of the boundary layer $\delta = L/(2 \cdot Nu)$. Thicknesses of the boundary layers for various Ra and Nu numbers are listed in Table 2. A height of 35 mm of the “thin sidewalls” was then chosen. On the other hand the lower the sidewall, the thinner it can be from a structural point of view.

Table 2 Estimated thickness of the boundary layers

Ra	10^5	10^7	10^9	10^{11}	10^{13}	10^{15}
Nu	4	18	75	311	1290	5351
δ [mm]	34	8	2	0.5	0.12	0.028

3.2.2 Copper plates

The plates of the convection cell are made of oxygen free high conductivity copper (OFHC copper from Outokumpu company). The plates are 300 mm in diameter and are 28 mm thick. The internal surfaces of the plates are machined by soft lathe-turning. The guaranteed roughness of the surfaces is $R_a = 1.6 \mu\text{m}$. This is one order of magnitude lower than the lowest thickness of the boundary layer at $Ra \sim 10^{15}$ (see Table 2). In fact, the roughness could influence the measured $Nu(Ra)$ dependence if it is comparable to the boundary layers thickness.

Once ready the plates were annealed in the vacuum furnace at 650 °C. The heat conductivity of these plates was determined by measuring the RRR (Residual Resistance Ratio). Samples for the measurement were cut off from the copper plates during lathe-turning and annealed together with plates. For the annealed sample the value of $RRR = 290$ was found. The heat conductivity of 1800 W/m/K (4.2 K) was determined from this RRR value.

3.2.3 Construction joints and the technology

The thin bottom sidewalls are connected to the copper plates via stainless steel rings (Figure 3). These are brazed to the copper plates on their external sides. Stainless steel sidewalls are microplasma welded to the rings.

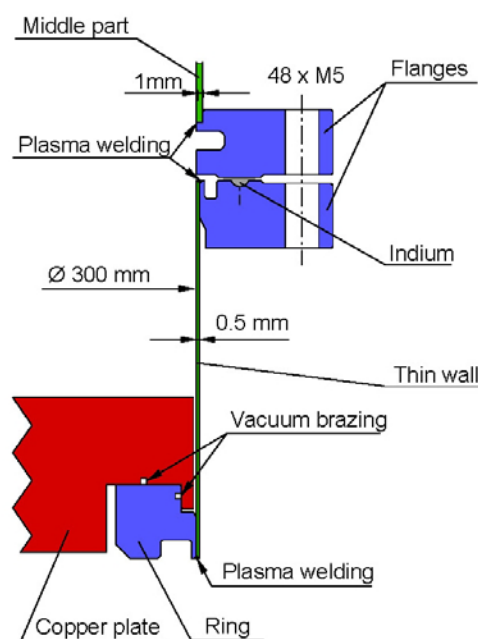


Figure 3 Design and technology of the joints

The bottom parts are connected to the middle part by demountable flanges. The joints of these flanges are sealed by indium wires.

The convection cell is connected to the LHe vessel via the heat exchange chamber by demountable flanges. The lower part of the heat exchange chamber is a component of the top part of the cell, the upper part is a component of the LHe vessel.

4 ANALYSIS OF THE CONVECTION EXPERIMENT

4.1 MEASUREMENT OF $NU(RA)$ DEPENDENCE

Adjustment of the Rayleigh number Ra can be achieved by varying the He fluid density, heat power Q_b (applied to the bottom plate) and temperature T_t of the top plate. He state is evaluated from the measured temperatures of the plates (i.e. from

their mean temperature T) and from the measured pressure in the cell. For the known state of He, the properties α , ν and κ are obtained from the NIST database [10], which is widely used as standard. The Rayleigh number Ra is then evaluated from Eq. (2).

The Nusselt number Nu is calculated from the measured temperature difference ΔT between the plates and heat power Q_b applied to the bottom plate, that is, from Eq. (1).

4.1.1 Measured quantities

Pressure measurement

The pressure p of the gas within the cell is measured by using a Baratron 690A 53T RB transducer with an absolute accuracy of about 0.08 %.

Heat power

The heat input to the bottom plate Q_b is measured by a four-wire technique with accuracy better than 0.5 %.

Temperature measurement

Temperatures of top and bottom copper plates, T_t and T_b , will be measured by calibrated germanium temperature sensors Lake Shore GR-200A-1500-1.4B with an absolute accuracy of 4 mK (uncertainty determined for 95 % coverage probability, i.e. coverage factor $k=2$). Thus the uncertainty of the mean temperature $T = (T_t + T_b)/2$ of the He fluids is about 3 mK.

It is planned to stabilise the temperature T_t of the top plate by using the temperature controller Lake Shore 340.

The accuracy of measurement of temperature difference ΔT in the cell was increased by additional comparative calibration of germanium temperature sensors of the top and bottom plates. The uncertainty 2 mK ($k=2$) of small values of ΔT was achieved.

4.1.2 Total accuracy assessment

In accordance to the theory outlined in (sec. 1.2.1), a scaling law $Nu \sim Ra^{1/3}$ is expected. This is equivalent to a constant value of the $Nu/Ra^{1/3}$ ratio.

For simplicity the Nu^3/Ra ratio is used for uncertainty analysis in this section, i.e.

$$\frac{Nu^3}{Ra} = \frac{\frac{Q_b^3}{\left(\lambda \cdot \frac{\Delta T}{L} \cdot S\right)^3}}{g \cdot \frac{\alpha \cdot \Delta T}{\nu \cdot \kappa} \cdot L^3} = \frac{1}{g \cdot S} \cdot \frac{Q_b^3 \cdot \sigma}{\Delta T^4}, \quad (7)$$

where

$$\sigma \equiv \frac{\nu \cdot \kappa}{\lambda^3 \cdot \alpha} \quad (8)$$

depends on the state of He fluid.

To test the validity of this law we need to know the accuracy of the Nu^3/Ra measurement. The relative uncertainty in this ratio caused by the uncertainties in the determination of individual quantities can be derived as

$$\rho\left(\frac{Nu^3}{Ra}\right) = \sqrt{[3 \cdot \rho(Q_b)]^2 + [4 \cdot \rho(\Delta T)]^2 + [\rho(\sigma)]^2}, \quad (9)$$

where

$$\rho(\sigma) = \sqrt{\left(\frac{\partial \sigma}{\partial T} \cdot \frac{\delta T}{\sigma}\right)^2 + \left(\frac{\partial \sigma}{\partial p} \cdot \frac{\delta p}{\sigma}\right)^2}. \quad (10)$$

The symbols ρ and δ stand for relative and absolute uncertainty, T is the mean temperature of the He fluid and p the pressure inside the cell.

A nearly constant $Nu/Ra^{1/3}$ ratio was observed by the Oregon group over a range of Ra values from 10^6 to 10^{15} . On the other hand, the Grenoble group published $Nu/Ra^{1/3}$ ratio which deviates up to about 40 % from the constant value within the range of Ra values from 10^8 to 10^{12} (Figure 4). This results in more than 100 % deviation in Nu^3/Ra ratio. Measurement accuracy of 20 % in Nu^3/Ra ratio (i.e. 7 % in $Nu/Ra^{1/3}$) was chosen as sufficient for distinguishing such a deviation from constant. Thus in the following text when we speak about “ratio Nu^3/Ra measured with sufficient accuracy” we mean that Nu^3/Ra ratio is characterised by uncertainty less than 20 %.

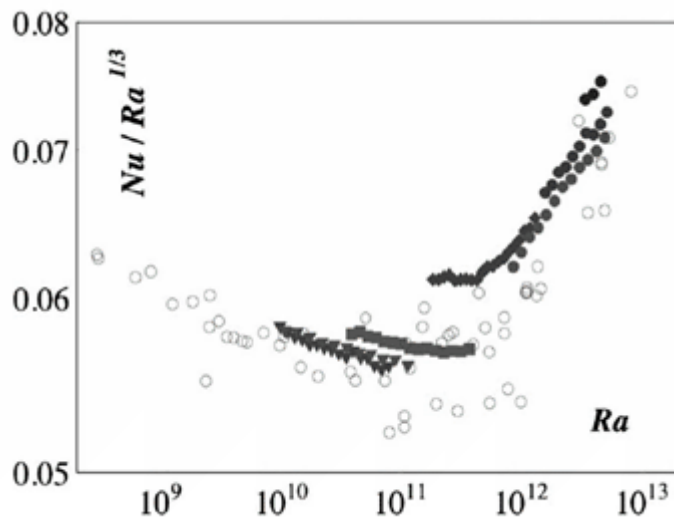


Figure 4 Experimental Ra dependence of $Nu/Ra^{1/3}$ measured by the Grenoble group [5]

4.2 MODEL OF THE EXPERIMENT

For the analysis of the convection experiment the SimRBC program was written by using Microsoft Office Excel [27]. Operation parameters for the convection cell, heat exchange chamber and LHe vessel and errors of the measured quantities are approximately predicted by the SimRBC program. The prediction was performed for scaling law with exponent $\gamma \sim 1/3$ published by Niemela et al [8]. This law was used for an estimate of the heat transferred both in the cell and heat exchange chamber. HePak add-in computer program for Excel [29], was used for the calculation of the thermophysical properties of He according to the NIST database [10].

4.2.1 Results of the analysis

Results of the simulation for various densities of He in the cell are presented in Figures (5-8) where the condition $\alpha \Delta T = 0.2$ was applied. Only results with the Nu^3/Ra ratio with sufficient accuracy to distinguish controversial results on scaling law are presented (sec. 4.1.2).

Uncertainties of Nu^3/Ra

The total relative uncertainty of the ratio Nu^3/Ra , see Eqs. (10-11), caused by uncertainties in the mean He temperature T (3 mK), pressure p (0.1 %), temperature difference ΔT (2 mK) and heat power (0.5 %) is shown in Figure (5).

The ΔT measurement is responsible for the highest contribution to the Nu^3/Ra uncertainty, even though Ge sensors were additionally calibrated one relatively to each other to increase the accuracy of the measured temperature difference ΔT .

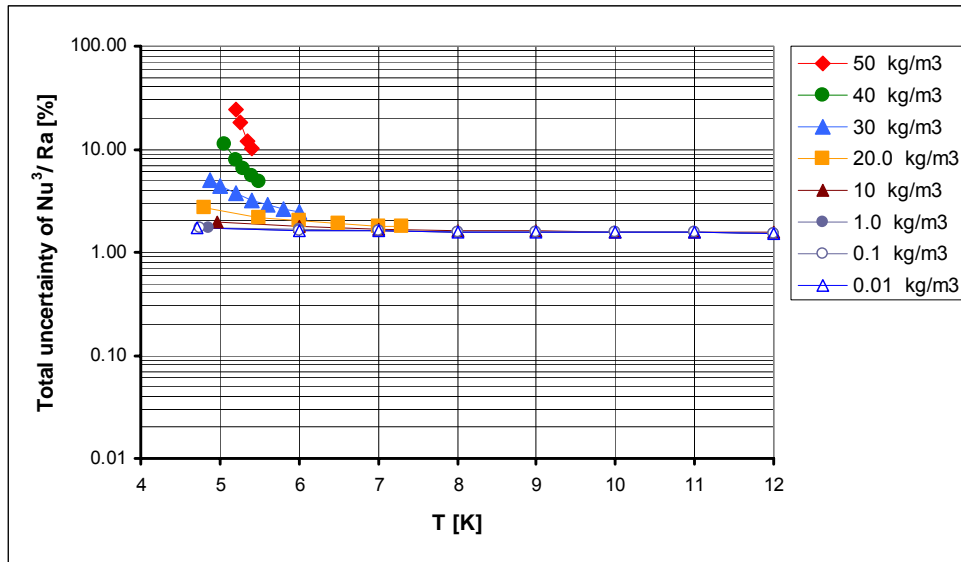


Figure 5 Dependence of the total relative uncertainty in the Nu^3/Ra ratio on the mean temperature T derived from Eq. (9) for various densities and caused by uncertainties in the determination of the mean He temperature T (3 mK), pressure p (0.1 %), temperature difference ΔT (2 mK) and heat power (0.5 %)

Ranges of Ra numbers and the measured quantities

The dependence of the Ra numbers, calculated from Eq. (2) on the mean temperature T and pressure p are plotted in Figure 6(a, b).

The highest $Ra = 2.3 \cdot 10^{14}$ in Figure 6(a, b) is predicted to be measured with a total uncertainty of the Nu^3/Ra ratio lower than 20 % with a 50 kg/m^3 He density. The higher value of $Ra = 10^{15}$ could be achieved with a density of He close to its critical point ($\sim 70 \text{ kg/m}^3$) but with an uncertainty of 50 % or to increase the temperature difference ΔT and to measure under non-Boussinesq conditions.

Ra numbers decrease with increasing temperature (Figure 6(a)). The maximum temperature at which convection can be studied is limited by the maximum operating pressure.

Ra numbers decrease with increasing pressure p for a given He density (Figure 6(b)). For design reasons, a lower pressure in the cell is preferred: the value of the maximum operating pressure of 250 kPa was chosen as sufficient for high Ra experiments.

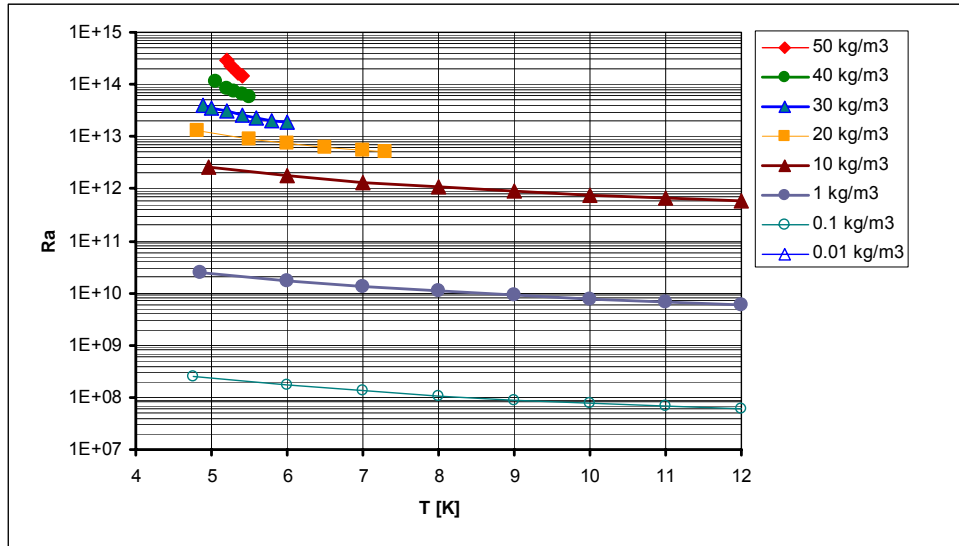


Figure 6 (a) Calculated Rayleigh number Ra dependence on the mean density and temperature T of He in the experimental cell ($L = 300 \text{ mm}$). For the prediction of Ra number values the Boussinesq condition $\alpha \cdot \Delta T = 0.2$ and the scaling law with exponent $\gamma \sim 1/3$ were used

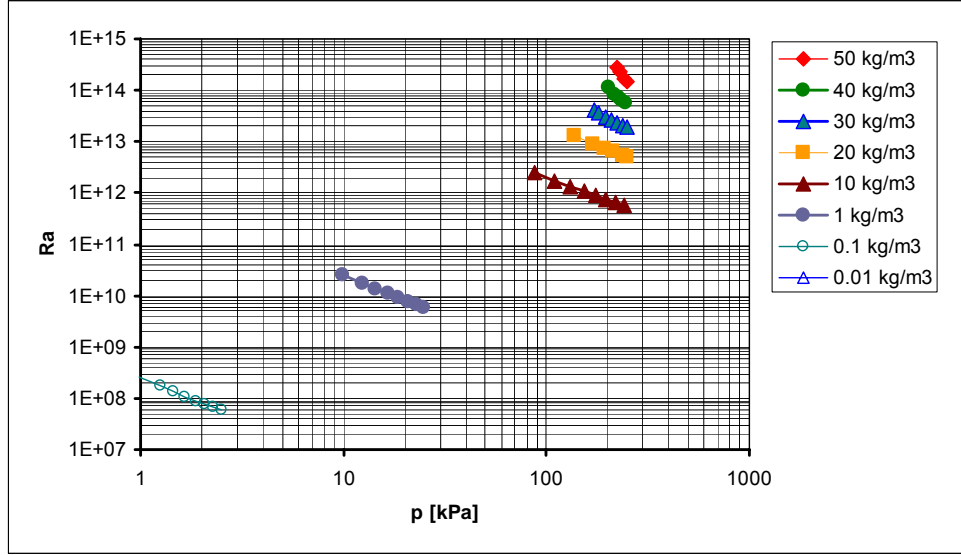


Figure 6 (b) Rayleigh numbers from Figure 6 (a) presented in dependence on He pressure p and mean density

For the highest densities ($10 \text{ kg/m}^3 - 50 \text{ kg/m}^3$), that is for highest values of Ra , the highest heat power to the bottom plate Q_b in the range from 1 W to 5 W is necessary when approaching a pressure of 250 kPa (Figure 7).

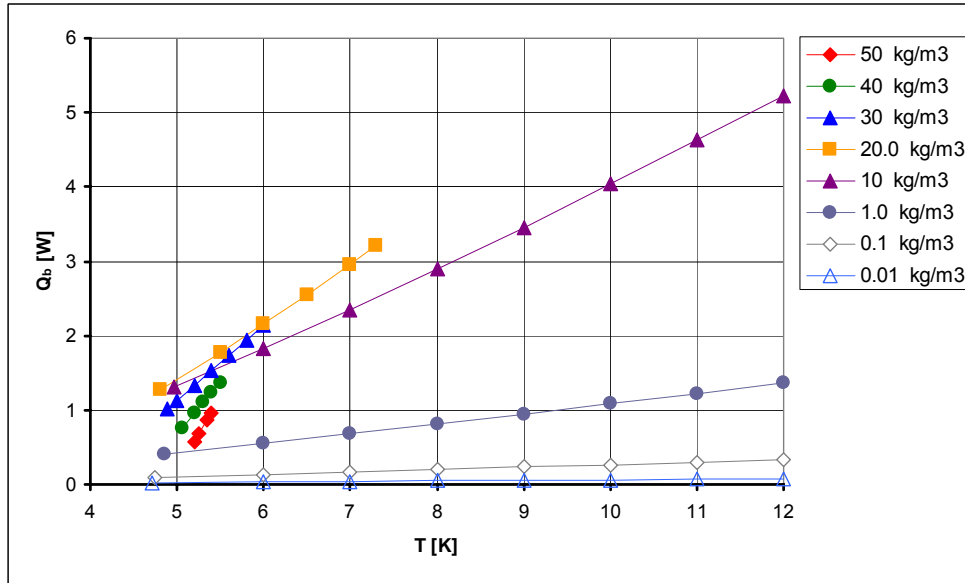


Figure 7 Dependence of the heat power Q_b to the bottom plate on the mean temperature T

Time of convection stabilization

The time constant

$$\tau = \frac{L^2}{2\kappa Nu} . \quad (11)$$

was derived for convection stabilization. The setting of the steady-state with an accuracy of 0.1 mK requires a time $t \sim 10\tau$. The time of steady-state setting increases with the He density in the cell and varies from minutes to hours, see Figure 8(a).

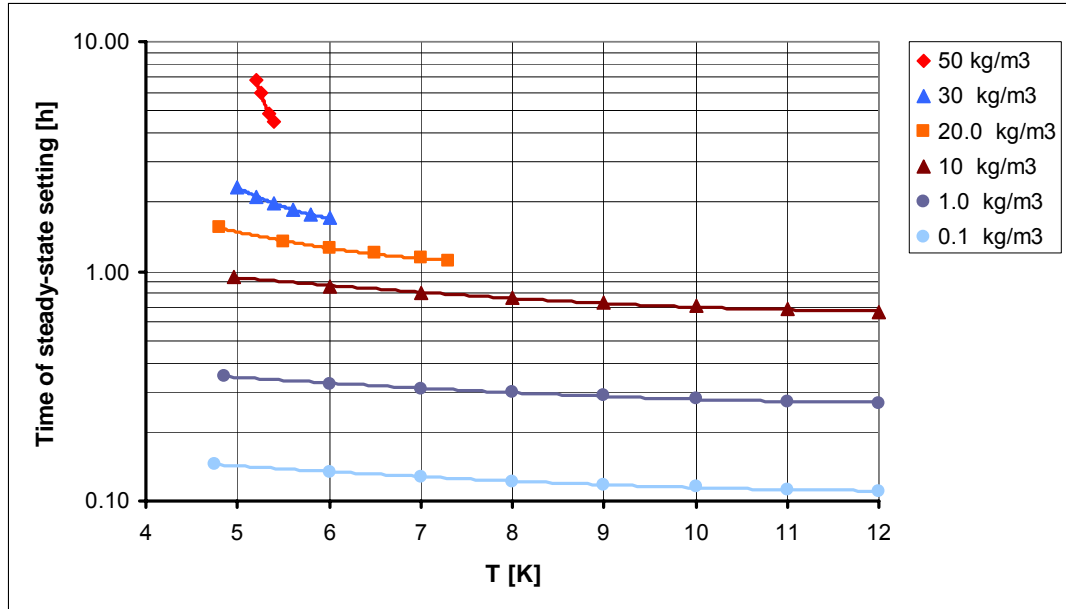


Figure 8 (a): Estimated time (10τ) for the setting of the steady-state temperature T_b at the bottom plate with an accuracy of about 0.1 mK

LHe consumption

The convective heat flux is transferred into the LHe vessel and evaporates LHe. The consumption of LHe increases with increasing density and temperature of He in the cell (Figure 8(b)).

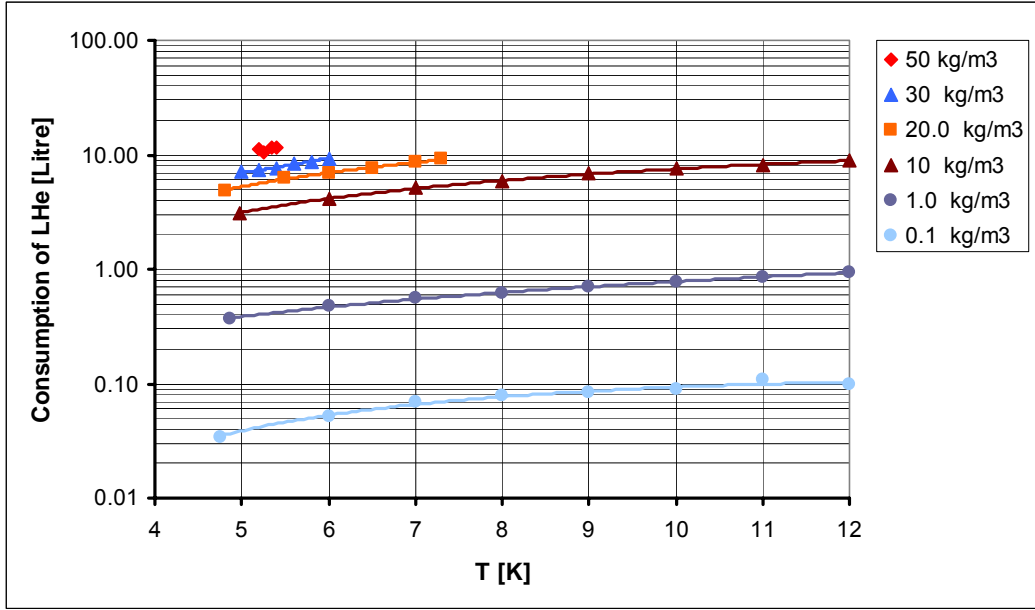


Figure 8 (b): Consumption of LHe during the time $t = 10\tau$ for the setting of the steady-state temperature T_b at the bottom plate with an accuracy of about 0.1 mK

The LHe consumptions are calculated for the time 10τ which is necessary to stabilize the convection. For $Ra = 1.5 \cdot 10^{14}$ (He density of 50 kg/m^3 at 5.4 K) the LHe consumption is 11.5 litres during the stabilization time of 4.5 h.

4.3 HEAT FLUX ANALYSIS OF THE CRYOSTAT

The heat flux analysis was performed to estimate parasitic heat fluxes to the vessels with cryoliquids (LN2 and LHe vessels) in the pause between experiments, when the plates are not heated. Another aim was to analyse parasitic heat fluxes to the convection cell during experiment.

The heat fluxes inside the cryostat were calculated by using the KRYOM software 3.3 [26], [28]. This program packet is based on numerical procedures developed for the thermal analysis of cryostats.

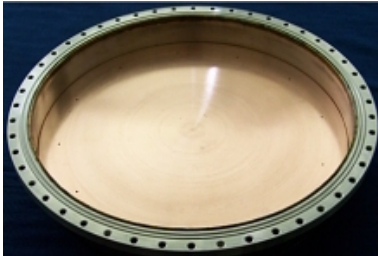
Results

The parasitic heat fluxes into the convection cell were minimized up to a value of 1 mW. At measurement of $Nu > 20$ ($Ra > 1E7$) the parasitic heat fluxes are less than 1 % of the convective heat flux. Total heat loads 60 mW to the LHe vessel and 5460 mW to the LN2 vessel were calculated.

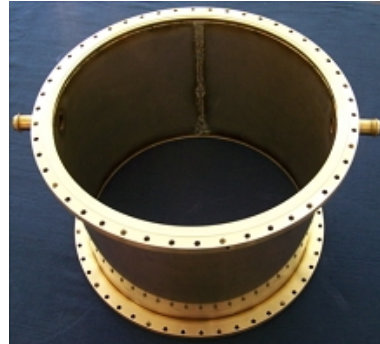
5 REALIZATION OF THE CRYOSTAT

5.1 THE CONVECTION CELL

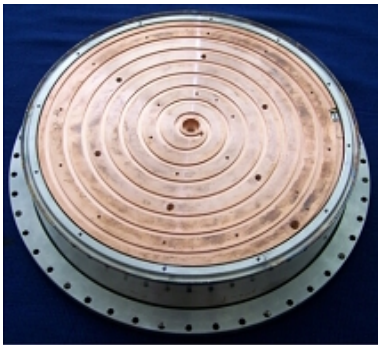
The bottom and middle parts of the cell can be seen in Figure 9.



a) Bottom part - internal side view



c) Middle part



b) Bottom part - external side view



d) Top part of the cell

Figure 9 Parts of the convection cell

The internal side of the bottom part is shown in Figure 9(a). The copper plate is machined by soft lathe-turning (roughness $R_a < 1.6 \mu\text{m}$). On its external side the groove is milled (Figure 9(b)) for a resistance heater and two holes are drilled here for two temperature sensors in the centre and at the margin of the copper plate. The middle part with parts of the filler necks and the top part of the cell with the lower part of the heat exchange chamber are shown in Figure 9(c-d).

The assembly of the whole convection cell, composed of the bottom, middle and the top parts, is illustrated in Figure 10.

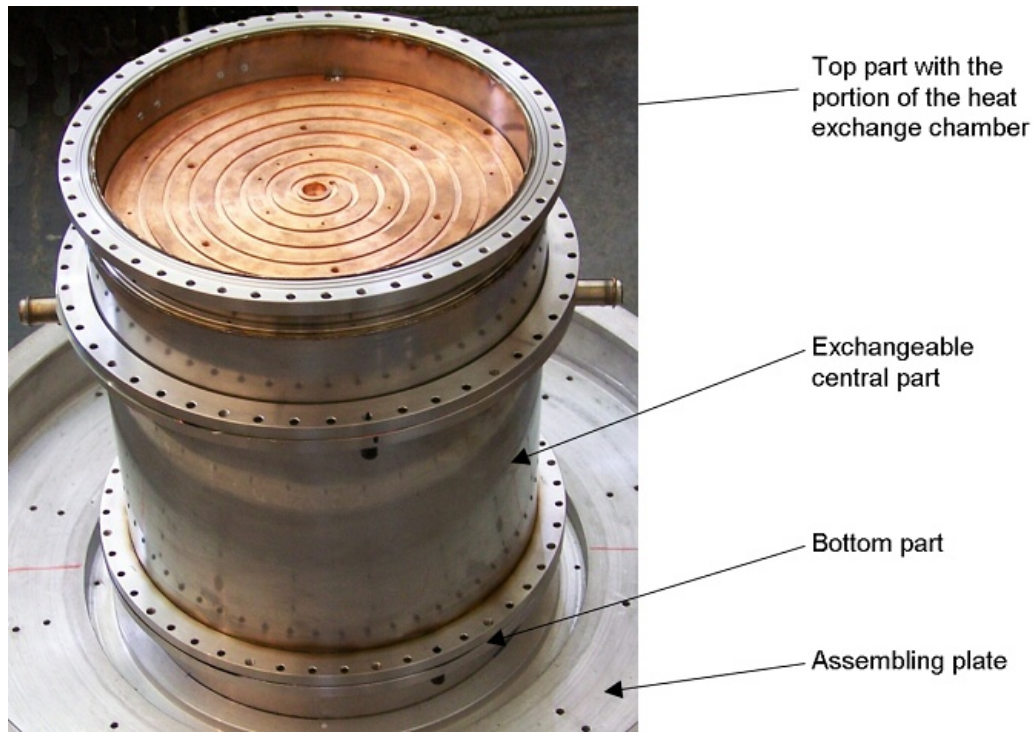


Figure 10 Assembly of the convection cell

5.2 LHe VESSEL

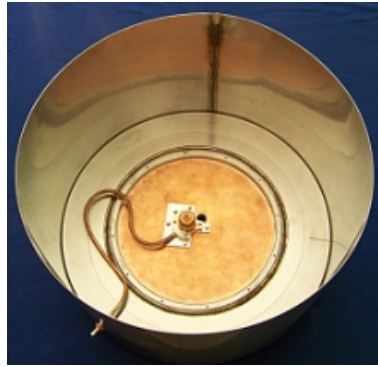
Assembly of the LHe vessel with a filling neck (central neck of the cryostat) is shown in Figure 11(a). The LHe vessel is made of stainless steel with exception of the bottom middle plate which is made of copper (Figure 11(b)).

The copper bottom part transfers the heat flux from the heat exchange chamber to the liquid in the LHe vessel. The upper part of the heat exchange chamber, which is a portion of the LHe vessel, is shown in Figure 11(c). The stainless steel bushing is vacuum brazed to the copper bottom part.

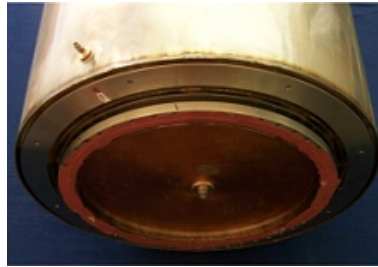
A liquid He valve is placed on the copper bottom part in the LHe vessel (Figure 11(b and d)). The convection cell will be filled by this valve during experiments. The valve is connected to the cell by a copper tube which passes through the cylindrical walls of the LHe vessel and leads to the cell middle part. The liquid He valve was specially designed and manufactured for this cryostat.



a) Assembly of the LHe vessel



b) View inside the LHe vessel



c) Bottom part of the LHe vessel, top part of the heat exchange chamber



d) LHe valve

Figure 11 Assembly and parts of the LHe vessel

5.3 CRYOSTAT ASSEMBLY

The cryostat assembly and dismantled cryostat, where the convection cell is visible, are shown in Figure 12.



Figure 12 Cryostat assembly

6 CONCLUSIONS

A helium cryostat with the cylindrical convection cell, 300 mm in both diameter and height, has been designed, manufactured, assembled and tested. The whole apparatus is ready for experiments on very high Rayleigh number turbulent convection, using cryogenic helium gas as a working fluid. The cell is designed for the experiment which ought to resolve the existing contradictions in various aspects of the convective flow and heat transport, especially in the scaling exponent of the $Nu(Ra)$ power law dependence (sec. 1.3.3), with the advantage of the so far minimal influence of the cell structure on the convection at both low and high ends of the attainable range of Ra numbers.

To achieve this goal, the convection cell was designed with especially thin sidewalls of as low as possible parasitic heat conductivity. The thin sidewall together with careful minimization of other parasitic heat fluxes (sec.4.3) reduces undesirable effects on the observed convection in the region of lower Ra values (sec. 1.3.4, 3.2.1 and 3.2.3). On the other hand, the use of the thick best available quality high-conductivity OFHC copper plates making the top and the bottom of the cell and additional annealing of them before installation minimizes any restrictive influence of the plates on convection at the upper end of attainable Ra (sec. 1.3.5 and 3.2.2).

Expected accuracy for the planned experiments has been evaluated based on:

- availability of commercially calibrated highly sensitive and stable Lake Shore Ge temperature sensors together with the ones additionally re-calibrated to increase the accuracy of measured temperature difference between plates
- high-precision Baratron pressure sensor calibrated (traceable to NIST standards) up to 500 kPa and corresponding read-out electronics
- cryogenic Lake Shore 340 temperature controller

The $Nu \sim Ra^\gamma$ scaling law for $20 < Nu < 4000$ can be measured with precision better than 7% for each individual point (uncertainty with covering probability 95%). We emphasize that the range $10^7 < Ra < 4 \cdot 10^{14}$ which corresponds to these Nu under assumption of γ near to 1/3 is sufficient to resolve the published controversies on the $Nu(Ra)$ scaling law (sec. 4.1.2 and 4.2.1).

This work has been conducted at the Institute of Scientific Instruments of the ASCR, v.v.i., Group of Cryogenics and Superconductivity.

7 REFERENCES

- [1] TRITTON, D. J. Physical fluid dynamics. 2nd edition. Oxford : Clarendon Press, 1988. – ISBN 0198544898.
- [2] SOMMERIA, J. The elusive ‘ultimate state’ of thermal convection. *Nature*, 1999, n. 398, pp. 294-295. – ISSN 0028-0836.
- [3] KRAICHNAN, R. H. Mixing-length analysis of turbulent thermal convection at arbitrary Prandtl number. *Physics of fluids*, 5, 1962, pp. 1374.- ISSN 0899-8213.
- [4] VERZICCO, R. ; SREENIVASAN, K. R. A comparison of turbulent thermal convection between conditions of constant temperature and constant heat flux. *Journal of fluid mechanics*, 2008, 595, pp. 203-219. – ISSN 0022-1120.
- [5] ROCHE, P. E. ; GAUTHIER, F. ; CHABAUD, B. ; HÉBRAL, B. Ultimate regime of convection : robustness to poor thermal reservoirs. *Physics of fluids*, 14, 2005, pp. 115107/1-4. – ISSN 0899-8213.
- [6] LOHSE D. ; TOSCHI, F. Ultimate state of thermal convection. *Physical review letters*, 90, 2003, no. 3, pp. 034502/1-3. ISSN 0031-9007.
- [7] SKRBEK, L. ; NIEMELA, J. J. ; DONNELLY, R. J. Turbulent flows at cryogenic temperatures : a new frontier. *Journal of physics : condensed matter*, 11, 1999, pp. 7761-7782. – ISSN 0953-8984.
- [8] NIEMELA, J. J. ; SKRBEK, L. ; SREENIVASAN, K. R. ; DONNELLY, R. J. Turbulent convection at very high Rayleigh numbers. *Nature*, 2000, n. 404, pp. 837-840. – ISSN 0028-0836.
- [9] ASHKENAZI, S. ; STEINBERG, V. High Rayleigh number turbulent convection in a gas near the gas-liquid critical point. *Physics review letters*, 83, 1999, pp. 3641 – 3644. – ISSN 0031-9007.
- [10] NIST Reference Fluid Thermodynamic and Transport Properties Database (REFPROP), Version 8.0, National Institute of Standards and Technology, USA (2000).
- [11] CHAVANNE, X. ; CHILLA, F. ; CHABAUD, B. ; CASTAING, B. ; CHAUSSY, J. ; HEBRAL, B. High Rayleigh number convection with gaseous helium at low temperatures. *Journal of low temperature physics*, 1996, vol. 104, n°1-2, pp. 109-129. – ISSN 0022-2291.
- [12] CHAVANNE X. ; CHILLA F. ; CASTAING B. ; HÉBRAL B. ; CHABAUD, B. ; CHAUSSY, J. Observation of the ultimate regime in Rayleigh-Bénard Convection. *Physical review letters*, 79, 1997, n. 19., pp. 3648-3651. – ISSN 0031-9007.
- [13] CHAVANNE X. ; CHILLA F. ; CHABAUD B. ; CASATING B. ; HEBRAL B. Turbulent Rayleigh- Bénard convection in gaseous and liquid He. *Physics of fluids*, 13 2001, n. 5, pp. 1300-1320. – ISSN 0899-8213.

- [14] GAUTHIER F. ; ROCHE P. E. Evidence of a boundary layer instability at very high Rayleigh number, EPL 83, 2008, 24005-p1-p6.
- [15] GAUTHIER F. ; SALORT, J. ; BOURGEOIS O. ; GARDEN J. L. ; DU PUIITS R. ; THESS A. ; ROCHE P. E. Transition on local temperature fluctuations in highly turbulent convection. EPL 87, 2009, 4406.
- [16] NIEMELA, J. J. ; SREENIVASAN, K. R. Confined turbulent convection, Journal of fluid mechanics, 2003, 481, pp. 355-384. – ISSN 0022-1120.
- [17] NIEMELA J. J. ; SREENIVASAN K. R. Turbulent convection at high Rayleigh numbers and aspect ratio 4. Journal of fluid mechanics, 2006, 557, pp. 411-422. – ISSN 0022-1120.
- [18] NIEMELA J.J. ; SREENIVASAN K. R. Formation of the "Superconducting" Core in Turbulent Thermal Convection. Physical Review Letters 100, 2008, Art. No. 184502. ISSN 0031-9007.
- [19] AMATI G ; KOAL K ; MASSAIOLI F ; SREEVANASAN K.R. ; VERZICCO R. Turbulent thermal convection at high Rayleigh numbers for Boussinesq fluid of constant Prandtl number. Physics of Fluids 17, 2005, 121701.- ISSN 0899-8213.
- [20] CALZAVARINI, E. ; LOHSE, D. ; TOSCHI, F. ; TRIPICCIONE, R. Rayleigh and Prandtl number scaling in the bulk of Rayleigh – Bénard turbulence. Physics of fluids, 17, 2005, n. 5, pp. 055107/1-7. – ISSN 0899-8213.
- [21] KUNNEN R. P. J. et al. Numerical and experimental investigation of structure/function scaling in turbulent Rayleigh-Bénard convection. Physical review, E 77, 2008, pp. 016302/1-13. – ISSN 1539-3755.
- [22] AHLERS, G. Effect of sidewall conductance on heat-transport measurements for turbulent Rayleigh-Bénard convection, Physical review, E 63, 2001, n. 2, pp. 145-154. – ISSN 1539-3755.
- [23] CHILLA F, RASTELLO M, CHAUMAT S, CASTAING B. Ultimate regime in Rayleigh-Bénard convection: The role of plates. Physics of fluids, 16, 2004, pp. 2452-2456.- ISSN 0899-8213.
- [24] ROCHE P. E. ; CASTAING B. ; CHABAUD B. ; HEBRAL B. ; SOMMERIA, J. Side wall effects in Rayleigh Bénard experiments. European Physical Journal, B 24, 2001, n. 3, pp. 405-408. – ISSN 1434-6028.
- [25] HANZELKA P. He kryostat NMR-III pro supravodivý magnet spektrometru NMR. In: Sborník přednášek VIII. školy fyziky a techniky nízkých teplot, Vysočina-Sykovec (ÚPT AV Brno), 1988, s. 44 – 45.
- [26] HANZELKA P. Numerical modelling in cryostat design: methods and experimental verification. Cryogenics 1993, 33(4):454-8.

Software

- [27] SimRBC, Microsoft Excell Workbook created at ISI AS CR, Group of Cryogenics and Superconductivity.

- [28] KRYOM 3.3, created at ISI AS CR, Group of Cryogenics and Superconductivity.
- [29] HEPAK, Thermophysical properties of Helium from 0.8 K or the Melting Line to 1500 K, Version 3.40 – Excell Add-In and Version 3.41 – ActiveX DLL, developed by Cryodata, Inc.

8 CURRICULUM VITAE

Pavel Urban

Born in Dačice, Czech Republic, on 26th December 1975

Education

2002 – present: Ph.D. student at Brno University of Technology, Faculty of Mechanical Engineering, Institute of Physical Engineering

Thesis: Physical Modelling of Turbulent Thermal Convection at Extremely High Rayleigh Numbers

1996 - 2001: Brno University of Technology, Faculty of Mechanical Engineering, Institute of Physical Engineering

Diploma thesis: Imaging of Aberration in the Particle Optics

Degree: Ing. (M.Sc. equivalent)

Work experience

2001 – present: Research worker, MRB Department, Institute of Scientific Instruments, Academy of Sciences of the Czech Republic

Participation in ISI Brno scientific programs:

- design of a cryostat for He turbulence measurement
- design and testing of a small helium cryopump for electron-optical devices
- measurement of active carbon characteristics for cryogenic devices
- measurement of a parasitic heat loads of He expansion turbines

2003 – present: Experiment “COMPASS” – CERN project No. NA 58 – operator of low temperature Li⁶D polarized target system (10 % of manpower capacity)

2003 (two months): Development of a cooling system for LN2 large amount bath under the boiling point, Applied Superconductivity Training and Research Advanced Centre (ASTRA), Institute of Electrical Engineering, Slovak Academy of Sciences, Bratislava, Slovakia

Abstrakt

V disertační práci je popsán heliový kryostat s experimentální válcovou konvekční celou pro studium proudění při přirozené konvekci za velmi vysokých Rayleighových čísel Ra (až do řádu 10^{15}) a Nusseltových čísel Nu (až do řádu 10^4). Pracovní látkou je studené ^4He , které umožňuje díky výhodným fyzikálním vlastnostem dosažení velmi vysokých hodnot čísel Ra . Návrh kryostatu je založen na koncepci láznových NMR kryostatů s nízkým odporem kryokapalin. Ve středu kryostatu je umístěna konvekční cela o průměru 300 mm a výšce 300 mm. Celu tvoří horní a spodní dno a výměnná střední část. Tyto díly jsou spojeny rozebíratelnými přírubami těsněnými indiovým drátem. Výměnná část umožňuje snadnou modifikaci geometrie cely. Hlavní přednost kryostatu spočívá v minimálním vlivu konstrukce cely a použitých materiálů na studovanou konvekci. Cela kryostatu je navržena pro pracovní tlaky do 250 kPa.

Abstract

The thesis focuses on the design of a helium cryostat with an experimental convection cell for the study of natural turbulent convection in the range of Rayleigh numbers Ra up to 10^{15} and Nusselt numbers Nu up to 10^4 . Cryogenic ^4He gas is used as a working fluid for experimental studies due to its advantageous properties that allow reaching very high Ra numbers. The cryostat design is based on the conception of low-loss NMR magnet cryostats. In the centre of the cryostat a cylindrical convection cell of 300 mm in diameter and 300 mm in height is placed. The cell is made of middle, top and bottom parts. These are jointed together by flanges sealed by indium wires. The middle part is exchangeable and allows the geometry of the cell to be modified. The cell is designed for measurements at pressures up to 250 kPa. The main advantage of this cryostat is the minimal influence of the cell design and materials on the studied convection.